Reduced Current Sensor Based Vector Controlled Synchronous Reluctance Motor Drive

Juhi Choudhary[1], Dr. Chandra Bhushan Mahato[2], and Dr. Taushif Ahmad[3]
[1.] *Department of Electrical Engineering, Aryabhatta Knowledge University, Patna*
[2.] *Department of Electrical Engineering, Government Engineering College, Bhojpur*
[3.] *Department of Electrical & Electronics Engineering, Nalanda College of Engineering, Chandi*

***Abstract*—In this study, the Maximum Torque/Ampere (MTPA) condition is used to operate the Synchronous Reluctance Motor (SynRM) drive. By reducing the machine's overall size, this control method increases the machine's efficiency per KW rating. For electric vehicles (EVs) powered by SynRM, this control approach works better. Reducing the current sensor required from two to one or none at all can lower the drive's overall cost and increase its acceptability for EV applications. Accordingly, the model-based current estimate technique for SynRM drives for EV applications is suggested in this work, completely doing away with the drive's requirement for current sensors. The suggested current estimation scheme's utility is confirmed in MATLAB/SIMULINK platform.**

***Index Terms*— dq0-frame, Electric Vehicle, MTPA Control, SynRM.**

I. INTRODUCTION

Electric motors use the majority of electrical energy generated globally. Electric motors come in a wide variety of design kinds. They usually go by different names [1] depending on their rotor structure and specific performance characteristics, such as squirrel cage induction motors, brushless DC motors, synchronous motors, switched reluctance motors, synchronous reluctance motors, permanent magnet synchronous motors, and induction motors. Rotor architectures based on the principles of reluctance torque have been theorized since the 1970s [1].

In the literature, motors that function on the basis of the reluctance torque concept are referred to as switched resistance motors (SRM) or synchronous resistance motors (SynRM). These two motor types differ in their architectures, characteristics, and rotor structure and control system. Despite the fact that SRMs are simple to manage, many applications do not prefer them due to their high torque ripples [1]-[5]. The SynRM idea was first proposed around the turn of the 20th century, but it has only recently begun to receive significant attention. Only recent advancements in rotor high-anisotropy design have allowed the SynRM to attain a higher efficiency despite benefits such its low cost, simple, and durable construction, cold rotor, a large field-weakening range, and the absence of pricey rare-earth metals [6]-[8].

Both the stator current and the rotor's absolute location and speed must be measured for feedback control. Several SynRM control techniques have been proposed in the literature [9]–[11]. One can achieve high dynamic performancethrough the application of vector control strategies such as stator-flux-oriented or rotor-oriented control systems [12]–[15]. Non-linear magnetic saturation events exist on both the direct (d-axis) and quadrature (q-axis) axes of SynRM [16] [17]. Control strategies have been developed to minimize the impact of stator windings on joule losses while optimizing torque output [18]. By using the control strategies, torque generation rises and stator winding losses decrease.

SynRM was commonly managed using the constant current angle control approach [19]. Maximum Torque Per Ampere (MTPA), Maximum Power Factor Control (MPFC), and Maximum Torque Per Flux (MTPF) are three possible methods for implementing this control scheme [20]. The MTPA control method was used in this investigation to achieve the motor's maximum torque. The motor's absolute rotor position needs to be determined in order to apply the SynRM control techniques.

Physical current sensors are used to measure the stator currents used in the inner current control loop (also known as the slave loop) and incremental encoders, absolute encoders, or resolvers are commonly used in industrial applications to measure the position of the rotor and, consequently, the rotor speed for the outer speed loop (also known as the Master loop) [21]. larger prices, a larger chance of malfunction, intricate wires,

and problems with electromagnetic interference that affect measurements are some of these sensors' disadvantages. By estimating the stator currents online using rotor speed and control voltage data, the use of current sensors is completely avoided in this work [1].

II. MATHEMATICAL MODELLING OF SYNCHRONOUSRELUCTANCE MOTOR

SynRM is multiphase machines which involve the application of reluctance torque. The stator-flux is controlled from the motor drive (stator side control). In SynRM, the rotor has no windings or electrically isolated from the stator. Rotor position is essential to operate the SynRM, that data can be either known from the estimation algorithm or position sensor.

The modeling of SynRM is similar to the 3 phase AC machines by using park-transformation. This method converts a balanced three-phase system to a two-dimensional machine. The complete stationary machine is transformed into the rotating reference frame with reference to rotor magnetic axis.

The magnetic axis of the three stator windings is shown in Fig.1 Three-dimensional coordinates A, B, C are transformed into two coordinate system called fixed reference frame (α-β axis/phase) and other two co-ordinate system called rotor reference frame (d-q axis). In α-β reference frame, the machine model even depends on rotor speed/position. But in the d-q axis, the model is simpler and very easy to develop a control system.

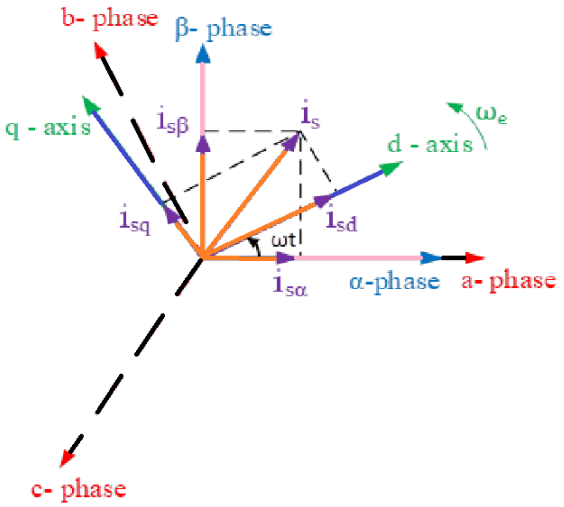

Fig. 1: Coordinate reference-frames for SynRM

The machine model in three phase reference frame is

$$\begin{bmatrix} v_a \\ v_b \\ v_c \end{bmatrix} = \begin{bmatrix} R & 0 & 0 \\ 0 & R & 0 \\ 0 & 0 & R \end{bmatrix} \begin{bmatrix} i_a \\ i_b \\ i_c \end{bmatrix} + \frac{d}{dt} \begin{bmatrix} \varphi_a \\ \varphi_b \\ \varphi_c \end{bmatrix} \quad (1)$$

where V_a, V_b, V_c represents the machine voltages, i_a, i_b, i_c represent each phase currents, R and φ denotes the per phase resistance and magnetic flux.

Voltage equations in rotor reference frame (dq-axes) can be expressed as

$$\frac{di_{ds}}{dt} = \frac{v_{ds}}{L_d} - \frac{i_{ds}R_s}{L_d} + \frac{\omega_e L_q i_{qs}}{L_d} \quad (2)$$

$$\frac{di_{qs}}{dt} = \frac{v_{qs}}{L_q} - \frac{i_{qs}R_s}{L_q} - \frac{\omega_e L_d i_{ds}}{L_q} \quad (3)$$

The space vector of stator current and the space vector of stator flux linkage interact to produce the electromagnetic torque. Since there is no rotor current, stator current alone is used to establish stator flux connections. The equation for electromagnetic torque is as follows:

$$T_e = \frac{3}{2} P(L_{ds} - L_{qs}) i_{ds} i_{qs} \quad (4)$$

The motor's mechanical equation is provided by:

$$J\frac{d}{dt}\omega_r = T_e - T_L - B\omega_r \quad (5)$$

where J represent moment of inertia and B represents co-efficient of viscous friction.

III. PROPOSED CURRENT ESTIMATION TECHNIQUE

Usually, in the closed loop vector control, we require two current sensors and a one-speed sensor for a balanced load. This method of current estimation of SynRM drive uses one current sensor with a one-speed sensor. So, the reduction of one current sensor will reduce the overall cost as well as our control drive becomes robust. The mathematical expression of the current estimation are as follows-.

$$v_{qs} = R_s i_{qs} + \omega_e L_{ds} i_{ds} + L_{qs} \dot{i_{qs}} \quad (6)$$

From above Eqn (6) we can find i_{qs} as

$$i_{qs} = \int \frac{v_{qs}}{L_{qs}} - \frac{R_s i_{qs}}{L_{qs}} - \frac{\omega_e L_{ds} i_{ds}}{L_{qs}}\, dt \quad (7)$$

This i_{qs} is taken as estimated i_{qs} that is, i_{qsest}

$$i_{qsest} = \int \left(\frac{v_{qs}}{L_{qs}} - \frac{R_s i_{qs}}{L_{qs}} - \frac{\omega_e L_{ds} i_{ds}}{L_{qs}} \right) dt \quad (8)$$

Since,

$$i_{s\alpha} = \sqrt{\tfrac{3}{2}}\, i_a \quad (9)$$

$$i_{\beta est} = i_{sd}^{*} \sin\theta + i_{qsest} \cos\theta \quad (10)$$

The complete block diagram of the proposed system is presented in Fig. 2.

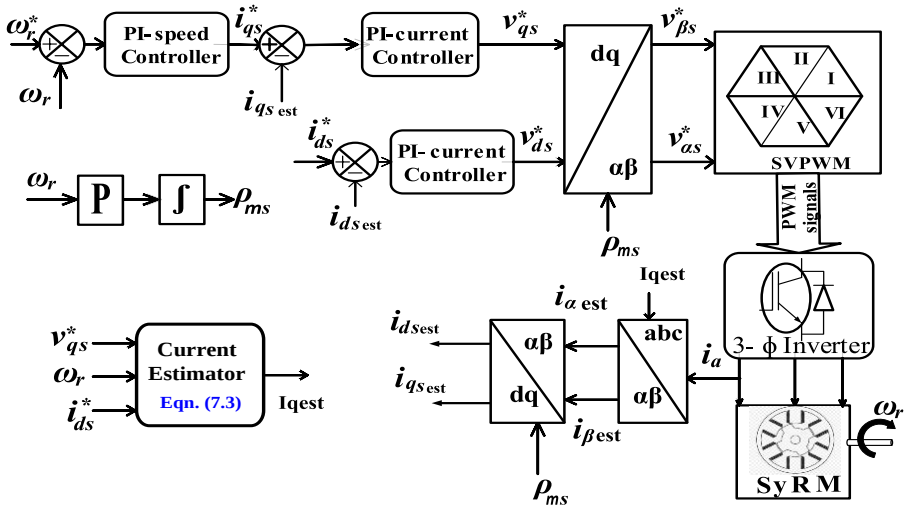

Fig 2: The complete block diagram of the current sensorless vector control SynRM drive

IV SIMULATION RESULTS

This section presents the simulation results for the current sensorless vector controlled SynRM drive, which is modelled using MATLAB/SIMULINK, for the different speed commands. Correspondingly output speed, torque, and currents (d-axis and q-axis) are measured.

A. Motoring Operation

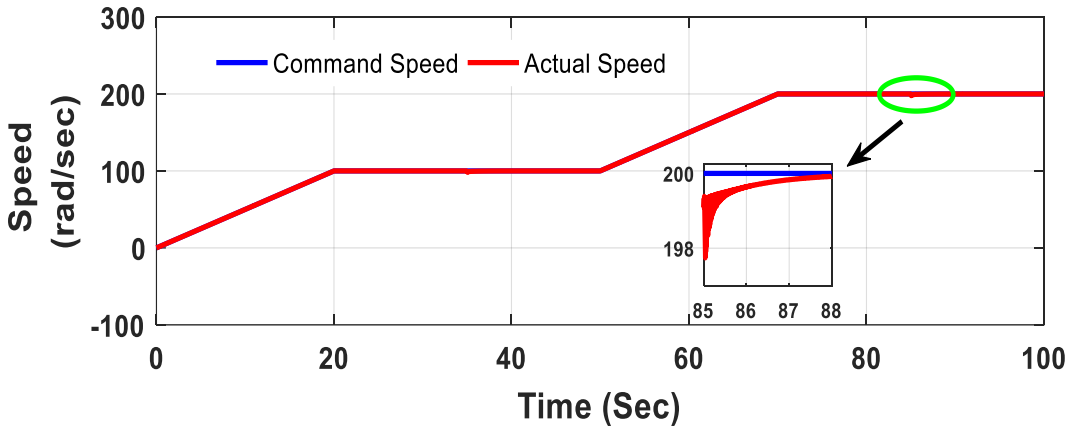

(a)

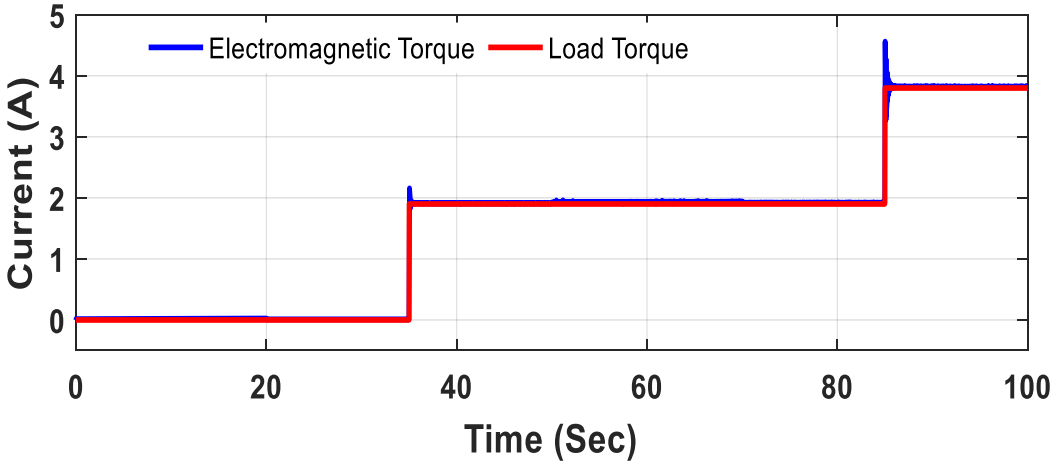

(b)

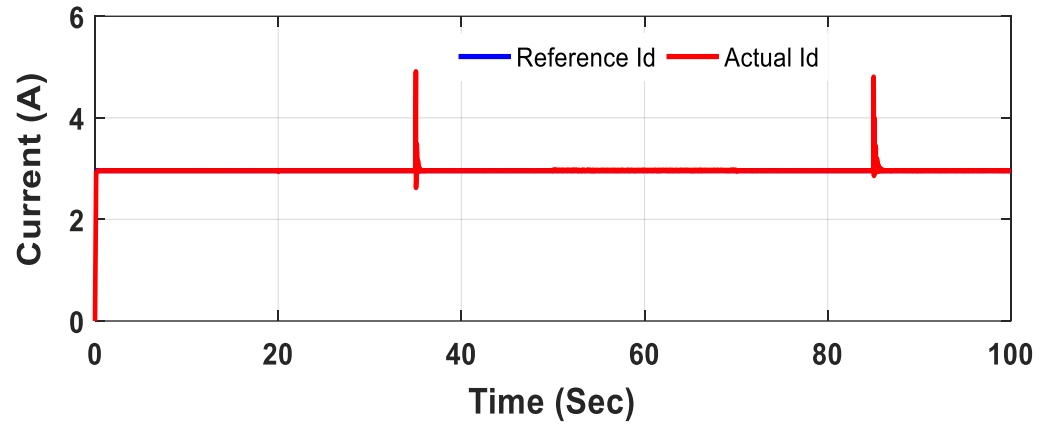
Reference Id
Actual Id
Current (A)
Time (Sec)
0
2
4
6
0
20
40
60
80
100

(c)

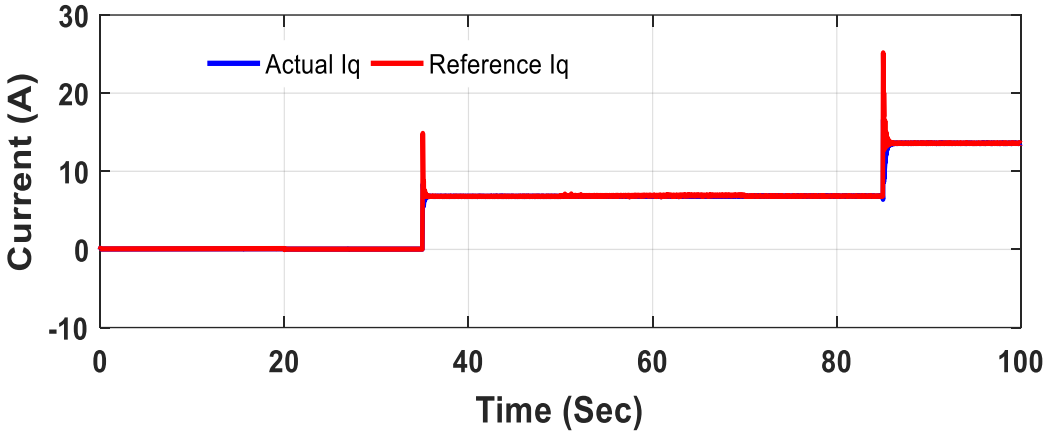
Actual Iq
Reference Iq
Current (A)
Time (Sec)
-10
0
10
20
30
0
20
40
60
80
100

(d)

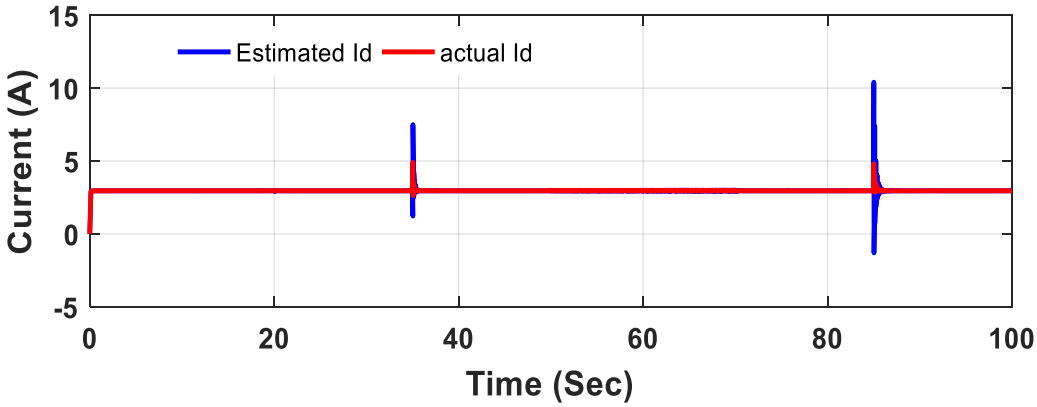
Estimated Id
actual Id
Current (A)
Time (Sec)
-5
0
5
10
15
0
20
40
60
80
100

(e)

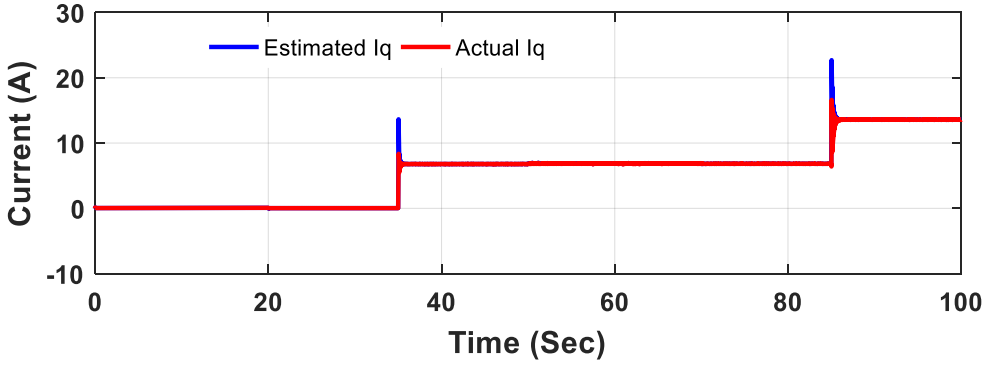
Estimated Iq
Actual Iq
Current (A)
Time (Sec)
-10
0
10
20
30
0
20
40
60
80
100

(f)

Fig. 3. Simulation results of current sensorless vector controlled SynRM drive: (a) Ramp change of speed in first quadrant (b) step change of torque (c) d- axis current (d) q-axis current (e) estimated d-axis current (f) estimated q-axis current

In this case, speed is given in the form of ramp signal (Fig. 3). The speed is changed from 0 to 100 rad/sec in 20 sec. From 20 sec to 50 sec the speed is maintained constant at 100 rad/sec. At 50 sec, the speed is changed from 100 rad/sec to 200 rad/sec in the form of ramp command. From 70 sec, the speed is maintained constant at 200 rad/sec till 100 sec. The reference and actual speed are presented in Fig. 3(a). Correspondingly the load torque is changed from 0 to 2 N-m at 35 sec in the form of step command. Further, the load torque is changed at 85 sec from 2 N-m to 4 N-m. The load torque and motor torque are presented in Fig. 3 (b). The reference and actual d-axis and q-axis currents are presented in Fig. 3(c) and Fig. 3 (d). Both the currents follow the reference current nicely. The estimated d-axis and q-axis currents follow the actual d-axis and q-axis currents without much error. This can be observed from Fig. 3 (e) and Fig. 3 (f).

B. Four Quadrant Operation

In this case, speed is given in the form of ramp signal (Fig. 4). The speed is changed from 0 to +200 rad/sec in 10 sec. From 10 sec to 30 sec the speed is maintained constant at +200 rad/sec. At 30 sec, the speed is changed from +200 rad/sec to -200 rad/sec in the form of ramp command. From 50 sec, the speed is maintained constant at -200 rad/sec till 70 sec. Further, the speed is changed from – 200 rad/sec to + 200 rad/sec in 20 sec and is then maintained constant at +200 rad/sec. The reference and actual speed are presented in Fig. 4 (a). Correspondingly the load torque is changed from 0 to +3 N-m at 20 sec in the form of step command. Further, the load torque is changed at 50 sec from +3 N-m to -3 N-m and then back to + 3 N-m at 90 sec. The load torque and motor torque are presented in Fig. 4 (b). The reference and actual d-axis and q-axis currents are presented in Fig. 4 (c) and Fig. 4 (d). Both the currents follow the reference current nicely. The estimated d-axis and q-axis currents follow the actual d-axis and q-axis currents without much error. This can be observed from Fig. 4 (e) and Fig. 4 (f).

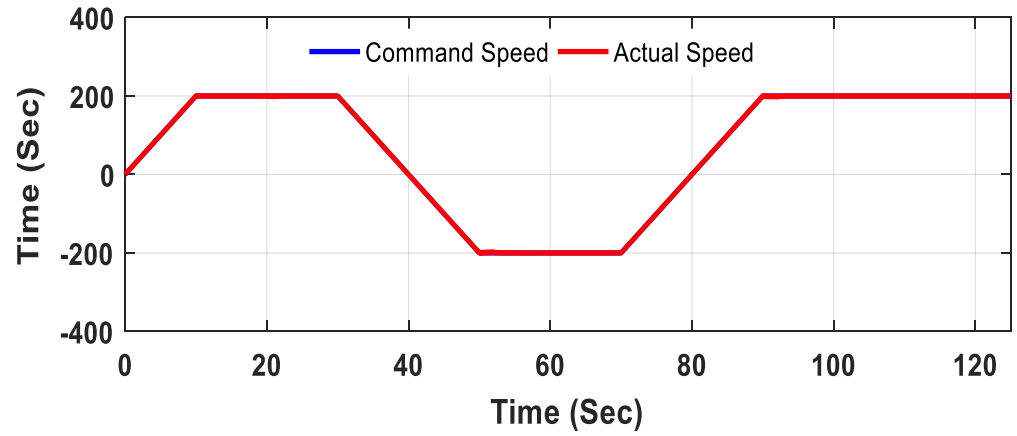

(a)

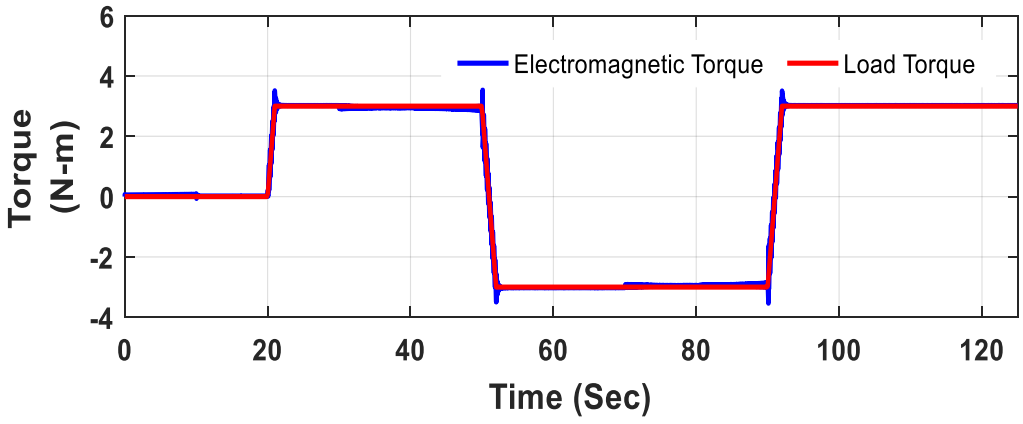

(b)

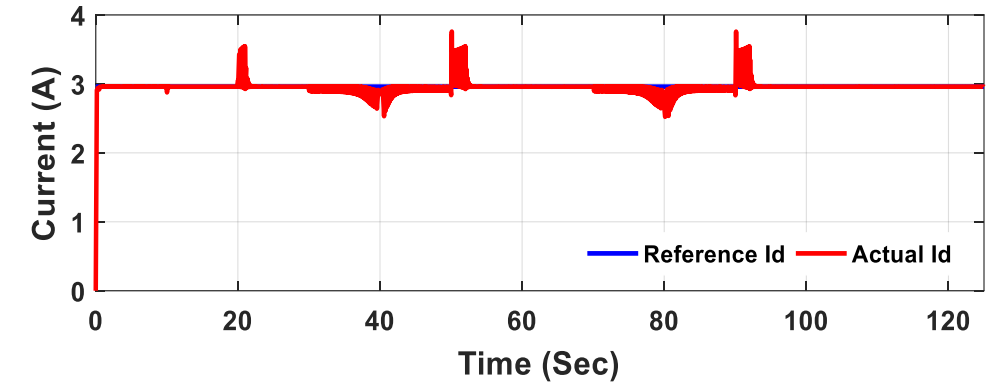
Current (A)
Time (Sec)
Reference Id
Actual Id

(c)

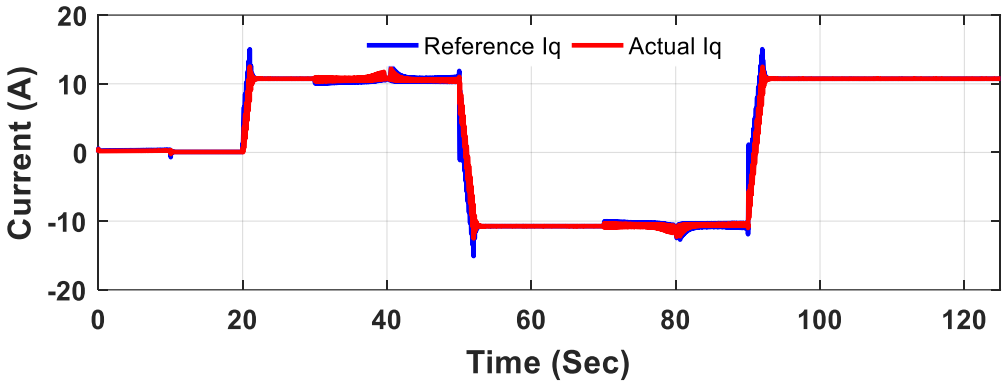
Current (A)
Time (Sec)
Reference Iq
Actual Iq

(d)

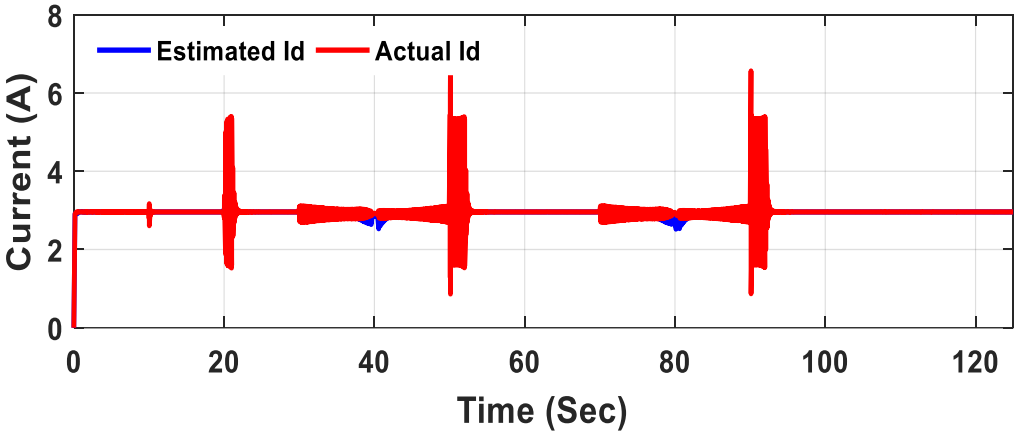
Current (A)
Time (Sec)
Estimated Id
Actual Id

(e)

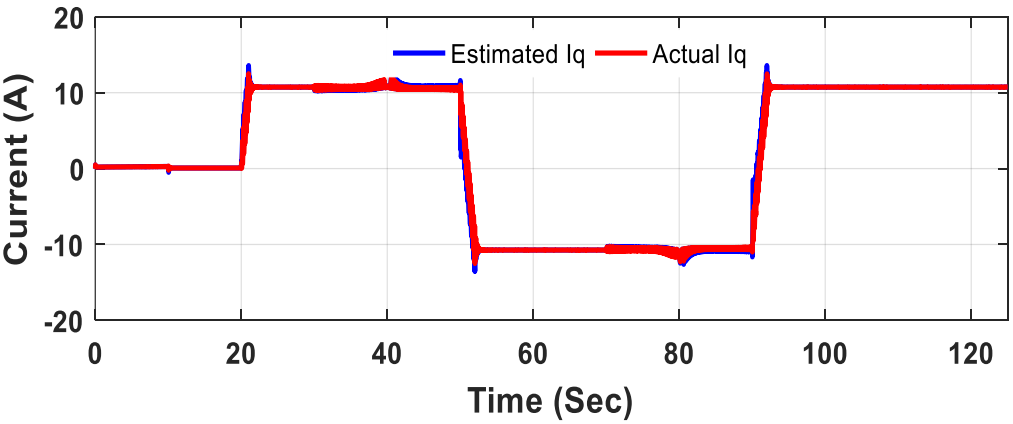
Current (A)
Time (Sec)
Estimated Iq
Actual Iq

(f)

Fig. 4. Simulation results of current sensorless vector controlled SynRM drive: (a) Ramp change of speed in four quadrant (b) step change of torque (c) d- axis current (d) q-axis current (e) estimated d-axis current (f) estimated q-axis current

Table I – Parameters of the SynRM

Rated Voltage	415 V
Speed	3000 rpm
Power	4.0 kw
Rated current	9.8 A
Rated Torque	12.7 N-m
Ld	72.92 mH
Lq	9.54 mH
R	1.034 ohm
No. of poles	2
J	0.00276 Kg-m2

V CONCLUSIONS

A vector-controlled SynRM drive based on a decreased current sensor is presented in this work. The current creation procedure for the d-q axis that is being given is completely independent of the switching states of the inverter. This was created using data from a single-phase current sensor and the rotating reference frame's d-axes reference current (ids*). The predicted two-phase currents can be used to rebuild three-phase currents. The drive's dependability on the existing sensors is decreased by the suggested technique. In order to make the vector-controlled SynRM drive fault-tolerant against current sensor failure, the suggested method lowers one of the current sensors in the drive and can be utilized to monitor the current sensor. Additionally, it works with all types of SynRM. Concurrent Reluctance The suggested approach is used to create a motor drive, which is then simulated using the MATLAB/SIMULINK platform.

REFERENCES

[1] R. Kumar, V. Verma, Y. A. Khan, and B. S. Shiva, “Q- MRAS based speed Sensorless vector controlled synchronous reluctance motor drive,” International Conference on Power Elect. App. and Tech. in Present Energy Scenario (PETPES), 29 Aug, 2019, pp. 1-6.

[2] A. Kumar, Y. A. Khan, and V. Verma, “Comparative Evaluation of PSO, TLBO, JAYA, Whale Optimization, and Grey Wolf Optimization Based Tuning of PI Controllers for Vector Controlled Synchronous Reluctance Motor Drive,” IEEE IAS (GlobConET), 20-22 May, 2022, pp. 261-266.

[3] G. Boztas, and O. Aydogmus, “Implementation of Sensorless speed control of synchronous reluctance motor using extended Kalman filter,” Engineering Science and Technology, an International Journal, vol. 31, 1 Jul, 2022, 101066.

[4] A. Farhan, M. Abdelrahem, C. M. Hackl, R. Kennel, A. Shaltout, and A. Saleh, “Advanced Strategy of Speed Predictive Control for Nonlinear SynRMs,” Machines, vol. 8, no. 3, 1 Aug, 2020, pp. 44.

[5] T. G. Woo, S. H. Lee, H. J. Lee, and Y. D. Yoon, “Flux Weakening Control Technique without Look-Up Tables for SynRMs Based on Flux Saturation Models,” Electronics, vol. 9, no. 2, 27 Jan, 2020, pp. 218.

[6] A. Farhan, M. A. Rahem, A. Saleh, A. Shaltout, and R. Kennel, “Simplified Sensorless Current Predictive Control of SynRM Using Online Parameter Estimation,” Energies, vol. 13, 2, 19 Jan, 2020, pp 492.

[7] Z. Mynar, P. Vaclavek, and P. Blaha, “Synchronous reluctance motor parameter and state estimation using extended Kalman filter and current derivative measurement,” IEEE Trans. on Industrial Electronics, vol. 68, no. 3, 25 Feb, 2020, pp. 1972-1981.

[8] C. Oprea, A. Dziechciarz, and C. Martis, “Comparative analysis of different synchronous reluctance motor topologies,” IEEE 15th Inter. Conf. on Environment and Electr. Eng (EEEIC), 10 Jun, 2015, pp. 1904-1909.

[9] H. C. Liu, and J. Lee, “Optimum design of an IE4 line- start synchronous reluctance motor considering manufacturing process loss effect,” IEEE Trans. on Indus. Elect., vol. 65 (4), 2 Oct, 2017, pp. 3104-3114.

[10] H. D. Lee, S. J. Kang, and S. K. Sul, “Efficiency- optimized direct torque control of SynRM using feedback linearization,” IEEE Trans. on Industrial Electronics, vol. 46, no.1, Feb, 1999, pp. 192-198.

[11] T. A. Lipo, “Synchronous reluctance machines-a viable alternative for ac drives,” Elect. Machines and Power Systems, vol. 19, no. 6, 1 Nov, 1991, pp. 659-671.

[12] R. Morales-Caporal, M. Pacas, “A predictive torque control for the SynRM taking into account the magnetic cross saturation,” IEEE

Trans. on Indus. Electronics, vol. 54 (2), 26 Mar, 2007, pp. 1161-1167.

[13] H. F. Hofmann, S. R. Sanders, and A. El-Antably, "Stator-flux-oriented vector control of SynRMs with maximized efficiency," IEEE Trans. on Indus. Electronics, vol. 51, no. 5, 4 Oct, 2004, pp. 1066-1072.

[14] L. Xu, X. Xu, T. A. Lipo and D. W. Novotny, "Vector control of a synchronous reluctance motor including saturation and iron loss," IEEE trans. on industry applications, vol. 27, no. 5, Sep, 1991, pp. 977-985.

[15] R. E. Betz, R. Lagerquist, M. Jovanovic, T. J. Miller, and R. H. Middleton, "Control of synchronous reluctance machines" IEEE Transactions on Industry Applications, vol. 29, no. 6, Nov, 1993, pp. 1110-1122.

[16] A. Vagati, M. Pastorelli, and G. Franceschini, "High- performance control of synchronous reluctance motors," IEEE Transactions on Industry Applications, vol. 33, no. 4, Jul, 1997, pp. 983-991.

[17] Y. Li, Z. Q. Zhu, D. Howe, and C. M. Bingham, "Modeling of cross-coupling magnetic saturation in signal-injection-based sensorless control of permanent- magnet brushless AC motors," IEEE Trans. on Magnetics, vol. 43 (6), 21 May, 2007, pp. 2552-2554.

[18] A. Vagati, M. Pastorelli, F. Scapino, and G. Franceschini, "Impact of cross saturation in synchronous reluctance motors of the transverse- laminated type," IEEE Transactions on Industry Applications, vol. 36, no. 4, Jul, 2000, pp. 1039-1046.

[19] A. Accetta, M. Cirrincione, M. C. Di Piazza, G. La Tona, M. Luna, and M. Pucci, "Analytical formulation of a maximum torque per ampere (MTPA) technique for SynRMs considering the magnetic saturation," IEEE Transactions on Industry Applications, vol. 56, no. 4, 11 May, 2020, pp. 3846-3854.

[20] G. Boztas, O. Aydogmus, and H. Guldemir, "Design and implementation of a high-efficiency low-voltage synchronous reluctance motor," Electrical Engineering, vol. 104, no. 2, Apr, 2022, pp. 717-725.

[21] P. R. Ghosh, A. Das, and G. Bhuvaneswari, "Performance comparison of different vector control approaches for a synchronous reluctance motor drive," 6th Intern. Conf. on Computer Appl. in Elec. Eng.- Recent Advances (CERA), 5 Oct, 2017, pp. 320-325.